Phytopathology® • 2023 • 113:1066-1076 • https://doi.org/10.1094/PHYTO-07-22-0257-R

Genetics and Genomics of Resistance

The In Planta Gene Expression of *Austropuccinia psidii* in Resistant and Susceptible *Eucalyptus grandis*

Shae Swanepoel,[1] Erik A. Visser,[1] Louise S. Shuey,[2] and Sanushka Naidoo[1,†]

[1] Department of Biochemistry, Genetics and Microbiology, Forestry and Agricultural Biotechnology Institute (FABI), University of Pretoria, South Africa
[2] Department of Agriculture and Fisheries, Queensland Government, Australia
Accepted for publication 21 December 2022.

Abstract

Austropuccinia psidii, commonly known as myrtle rust, is an obligate, biotrophic rust pathogen that causes rust disease in a broad host range of Myrtaceae species. *Eucalyptus grandis*, a widely cultivated hardwood Myrtaceae species, is susceptible to *A. psidii* infection, with this pathogen threatening both their natural range and various forest plantations across the world. This study aimed to investigate the *A. psidii* transcriptomic responses in resistant and susceptible *E. grandis* at four time points. RNA-seq reads were mapped to the *A. psidii* reference genome to quantify expressed genes at 12 h postinoculation and 1, 2, and 5 days postinoculation (dpi). A total of eight hundred and ninety expressed genes were found, of which 43 were candidate effector protein genes. These included *rust transferred protein 1* (*RTP1*), expressed in susceptible hosts at 5 dpi, and a hydrolase protein gene expressed in both resistant and susceptible hosts over time. Functional categorization of expressed genes revealed processes enriched in susceptible hosts, including malate metabolic and malate dehydrogenase activity, implicating oxalic acid in disease susceptibility. These results highlight putative virulence or pathogenicity mechanisms employed by *A. psidii* to cause disease, and they provide the first insight into the molecular responses of *A. psidii* in *E. grandis* over time.

Keywords: *Austropuccinia psidii*, dual RNA-seq, *Eucalyptus grandis*, host–pathogen interactions, oxalic acid, phytohormones

Austropuccinia psidii (Winter) Beenken (Beenken 2017) is an obligate biotrophic rust pathogen that causes myrtle rust on a broad host range within Myrtaceae, affecting approximately 480 species within 86 genera (Soewarto et al. 2019). Myrtle rust is considered a global pandemic, with incidence reports in North America, South America, Asia, Africa, and various Oceania countries (Carnegie et al. 2010; Coutinho et al. 1998; du Plessis et al. 2017, 2019; Giblin 2013; Kawanishi et al. 2009; Marlatt and Kimbrough 1979; McTaggart et al. 2016; Rayachhetry et al. 1997; Roux et al. 2016; Uchida et al. 2006; Zhuang and Wei 2011). Myrtle rust causes significant damage to growing plant leaves and shoots, causing shoot tip dieback, stunted growth, and in cases of severe infection, seedling death (Glen et al. 2007). Symptoms are known to vary within and between species, with some species displaying complete resistance, whereas others exhibit severe susceptibility (Minchinton et al. 2014).

Eucalyptus grandis is an important forestry species, valued for its wood quality and rapid growth properties (Grattapaglia et al. 2012). This economically and ecologically important hardwood species is vulnerable to various emerging pests and pathogens, including myrtle rust, which causes widespread losses to its natural and economic range. *E. grandis* is considered highly susceptible to myrtle rust infection, although some variation in disease severity exists between different genotypes (Junghans et al. 2003a). Constitutive expression of genes related to salicylic acid (SA)-mediated responses, photosynthesis, and a plethora of leucine-rich receptors was linked to resistance against myrtle rust in *E. grandis*, while these responses were limited or absent in susceptible samples (Santos et al. 2020). A recent study that combined proteomics and metabolomics to investigate the interactions between *A. psidii* and *E. grandis* implicated the phenylpropanoid pathway, photosynthetic pathway, and oxidative burst in the observed resistance against this pathogen (Sekiya et al. 2021). Plants susceptible to myrtle rust were found to exhibit similar responses, although earlier accumulation in resistant plants and more effective downstream control are the main factors separating the phenotypes (Sekiya et al. 2021). dos Santos et al. (2019) showed the importance of the cuticular waxes composition in the resistance against myrtle rust, with resistant plants having greater amounts of waxes than susceptible varieties. Moreover, susceptible *E. grandis* waxes contained hexadecenoic acid, and this compound was found to be favorable to *A. psidii*, impacting growth and germination.

There have been advances in our understanding of the putative mechanisms underlying host resistance against myrtle rust based on transcriptomic studies. Comparatively, few studies have investigated the mechanisms *A. psidii* employs to initiate host colonization and disease. Quecine et al. (2016) highlighted the importance of cell wall degrading enzymes (CWDEs) in the success of *A. psidii*, with enzymes such as peptidases, proteases, and modification proteins involved in host susceptibility. These authors found that susceptible guava (*Psidium guajava*) infected with myrtle rust had a greater

†Corresponding author: S. Naidoo; sanushka.naidoo@fabi.up.ac.za

Author contributions: S.S. performed data analysis, interpretation of results, and drafted the manuscript. E.A.V. assisted with data analysis, interpretation, and drafting of the manuscript. L.S.S. conceived of the study, performed experiments to obtain the data, and evaluated the manuscript. S.N. conceived of and obtained funding for the study, assisted in interpreting the biological responses, and drafting of the manuscript. All authors approved the submitted version.

Data have been uploaded to NCBI under bioproject PRJNA763498.

Funding: Support was provided by the South African National Research Foundation Y-rated grant to S. Naidoo (grant UID105767) and postdoctoral support to L. S. Shuey. Funding was also provided by the Technology Innovation Agency of South Africa through the Forest Molecular Genetics Cluster Program to S. Naidoo, S. Swanepoel, and E. A. Visser. Opinions and conclusions described herein do not reflect those of the National Research Foundation and other funding agencies.

e-Xtra: Supplementary material is available online.

The author(s) declare no conflict of interest.

abundance of pathogen-derived heat shock proteins (HSPs), tubulin, and actin proteins than what was found in the more resistant infected *E. grandis*, suggesting an involvement of these chaperones in maintaining pathogen virulence.

Rust fungi are a complex group of plant pathogens that consist of approximately 8,000 species (Aime et al. 2017). These diverse fungal pathogens have significantly larger genomes than any other fungal species, with sizes ranging from 300 Mbp to 2 Gbp (Aime et al. 2017; Bakkeren and Szabo 2020). Studies on rust pathogens have revealed candidate effector proteins, although to date, few of these have been functionally characterized (Petre et al. 2014). A rust pathogen of poplar (*Melampsora larici-populina*) secretes an effector protein (Mlp124357) that increases host susceptibility to bacterial and oomycete pathogens by localizing to the tonoplast of host cells to facilitate infection (Madina et al. 2020). A rust transferred protein (RTP1) was identified from the broad bean rust pathogen, *Uromyces fabae* (Kemen et al. 2005), and was found to form filaments inside the host plant to facilitate pathogen virulence during late-stage rust infection by protecting the haustorium from degradation (Kemen et al. 2013). Despite limited understanding of fungal effectors, and even more so of rust fungal effectors, recent advances in "omics" have facilitated studies on these complex organisms to unravel the role these proteins play during host colonization and fungal proliferation.

There have been few studies investigating the molecular interactions of myrtle rust within its host plants, highlighting the need for resources that can advance our understanding of the mechanisms by which this pathogen causes disease. With the release of the *A. psidii* reference genome (Edwards et al. 2022; Tobias et al. 2021), it is expected that many studies will emerge investigating this pathosystem. The identification of candidate effectors and virulence and pathogenicity genes highlights targets for future functional studies. The aim of this study was to investigate *A. psidii* responses in both resistant and susceptible *E. grandis*, to identify candidate effector proteins, as well as pathways involved in the interactions. Elucidating the molecular mechanisms that govern these interactions will highlight novel pathogen targets for disease control and management. This is the first study to look at the molecular interactions of myrtle rust with *E. grandis* over a time series.

Materials and Methods

A. psidii inoculation trial

E. grandis seedlings were sourced from wild plants across their natural distribution in eastern Australia, ranging from Coffs Harbour in New South Wales to northern tropical regions of Queensland. Seedlings were grown from seed and germinated in glasshouse conditions, where temperatures ranged from 20 to 30°C. The seedlings, all with at least four young leaves, were initially inoculated to determine the phenotypes. Inoculations were as reported in Swanepoel et al. (2021). The seedlings were screened for resistance and susceptibility on a scale of 1 to 5 at 2 weeks postinoculation, where seedlings rated one were considered resistant (R-interaction) and seedlings rated five were considered susceptible (S-interaction), based on the system used in Junghans et al. (2003b). Seedlings rated R and S were selected, and diseased tissues were removed. The seedlings were allowed to reshoot for 8 weeks. Seedlings were inoculated (infected) with *A. psidii* urediniospores in 0.05% Tween 20 with a concentration adjusted to 1×10^5 ml^{-1} or mock-inoculated with 0.05% Tween 20 (control) (Swanepoel et al. 2021). Samples were collected from these seedlings at four time points (12 h postinoculation [hpi] and 1, 2, and 5 days postinoculation [dpi]), with three replicates per time point per phenotype, and 14 seedlings per replicate.

Data generation and annotation

Total RNA extraction was performed on inoculated and mock-inoculated frozen leaf samples as described by Naidoo et al. (2013) and Swanepoel et al. (2021). Purified RNA from three biological replicates were submitted to the Beijing Genomics Institute (BGI) for mRNA-sequencing using 50-bp paired-end Illumina HiSeq 2500, an insert size of 300 bp, and a sequencing depth of 40 million reads per sample.

The host (Myburg et al. 2014) and pathogen (Tobias et al. 2021) reference genomes were downloaded from Phytozome v12.1.5 (Goodstein et al. 2011) and Zenodo (https://zenodo.org/record/3567172#.ZDBPdHbMLZt), respectively. The reference genomes were combined to create a genome index to be used in the mapping analysis. Quality filter-passed reads were mapped to the index genome using Spliced Transcript Alignment to a Reference (STAR) v2.7.0, a universal RNA-seq aligner tool (Dobin et al. 2013), and read counts were determined using StringTie v1.3.4d (Pertea et al. 2015). Read counts were imported into R v1.4.1106 (R Core Team 2018) using tximport v1.180 (Sonesone et al. 2015). The Eukaryotic non-model Transcriptome Annotation Pipeline (EnTAP) v0.8.2 (Hart et al. 2019) was used to obtain functional annotations of the myrtle rust genome. Diamond v0.9.9 (Buchfink et al. 2015) was used to perform BLASTp similarity searches using the NCBI nonredundant protein database, RefSeq complete protein database, and the UniProtKB/Swissprot database with a minimum-query coverage of 80%, minimum target coverage of 60%, and a minimum e-value of 1e–05. To obtain functional gene descriptions and gene ontology (GO) terms for each *A. psidii* gene, EggNOG v0.99.1 (Huerta-Cepas et al. 2019) and InterProScan v5.25-64.0 (Jones et al. 2014) were used. To identify putative pathways involved in the *A. psidii* infection process, the protein sequences of the expressed *A. psidii* genes were annotated using GhostKOALA (Kanehisa et al. 2008) and analyzed using the Kyoto Encyclopedia of Genes and Genomes (KEGG) database.

Differential expression analysis

To identify confidently expressed *A. psidii* genes, transcripts with read counts lower than 20 in at least three libraries were filtered out, as they are considered lowly expressed. The filtered read counts were analyzed using DESeq2 v 1.30.1 (Love et al. 2014). Pathogen genes with a Benjamini-Hochberg false discovery rate (FDR) of $P < 0.05$ and absolute $\log_2$(fold change) >0.5 were considered as significantly differentially expressed genes (DEGs). Comparisons between R- and S-interactions at each time point were made, where up-regulation refers to genes with greater expression in the S-interaction, and down-regulation refers to genes with lower expression in the S-interaction.

Functional characterization and identification of virulence and pathogenicity factors

To identify overrepresented gene ontology (GO), biological process (BP), cellular component (CC), and molecular function (MF) *A. psidii* terms, DEGs separated into up- and down-regulated genes were used for GO enrichment using GOSeq v1.42.0 (Young et al. 2010) with a Benjamini–Hochberg FDR of $P < 0.1$. Similarly, total expressed *A. psidii* genes separated into R- and S-interactions specific expression across the time series were used for GO enrichment following the same method. GO enrichment was determined separately for BP, CC, MF, and KEGG terms. To identify putative virulence and pathogenicity factors, expressed myrtle rust genes in the R- and S-interactions throughout the time series were identified and aligned to the pathogen–host interaction (PHI) database v4.2 (Urban et al. 2020), with a minimum e-value of 1e–04 and a minimum identity of 60% to the query sequence. Additionally, the expressed genes were compared with the candidate effectors identified by Tobias et al. (2021) in the R- and S-interactions throughout the time series. The protein sequences of the expressed candidate effectors were aligned to the NCBI nonredundant protein database with default parameters. Informative hits with a minimum e-value of 1e–05 were selected for further analyses.

Comparisons between *A. psidii* transcriptome and proteome data

In a previous study investigating the proteome of *A. psidii* in susceptible *P. guajava* and resistant *E. grandis*, urediniospores were collected from infected fruit and leaves of *P. guajava* and *E. grandis*, respectively (Quecine et al. 2016). The authors determined the protein abundance of these samples, and log ratios of susceptible relative to resistant abundance was made. Protein sequences of the 340 total detected proteins captured within the urediniospores were retrieved from the UniProtKB/Swiss (release Version 2021_04, https://www.uniprot.org/) with their accessions (Quecine et al. 2016). The protein sequences were used to perform a conditional reciprocal best (CBR) BLAST (Aubry et al. 2014) against the predicted *A. psidii* proteome to identify hits that are the most likely representatives of the previously identified proteins. These were then compared with the total expressed *A. psidii* genes to determine which proteins corresponded with expressed genes.

Results

RNA sequencing, mapping, and expressed *A. psidii* genes

RNA sequencing libraries for both the R- and S-interactions included approximately 20 million paired-end reads per sample at each time point (Supplementary Table S1). As expected, effectively 100% of mapped reads in the mock-inoculated control samples (con) mapped to the host reference genome for both R- and S-interactions at each time point, confirming the quality of the mapping analysis. Across the inoculated (inf) R- and S-interactions at each time point, 99.28 to 100% of mapped reads mapped to the host reference genome and 0.00 to 0.72% of mapped reads mapped to the pathogen reference genome. At 2 and 5 dpi in the resistant interaction, one and two biological replicates, respectively, as well as at 2 dpi in the susceptible interaction, less than 1,000 reads mapped to the pathogen genome. The overall lowly mapped pathogen reads may affect downstream gene expression analysis, as the number of mapped reads may not accurately represent the in planta interaction between *E. grandis* and *A. psidii*. More reads mapped to the S-interaction at 5 dpi than the R-interaction (Supplementary Table S1; Fig. 1). This is expected, as the S-interaction had significantly more disease symptoms than that of the R-interaction, and this may correlate with greater fungal biomass as the disease progresses in the S-interaction, resulting in the detection of more fungal RNA.

There were a total 890 confidently expressed *A. psidii* genes detected throughout the R- and S-interactions over the time series, with 683 having annotations (approximately 77%). Four hundred and twenty-four of the annotated genes had hits to hypothetical proteins (approximately 62%), and 26 genes had hits to uncharacterized proteins (approximately 4%). The remaining genes had informative annotations that may shed light on the interactions between myrtle rust and *E. grandis*. Figure 1 shows the distribution of expressed genes across the time series. There were more expressed genes detected in the S-interaction at 12 hpi, with 418 compared with 380 in the R-interaction. The number of expressed *A. psidii* genes increased in the R-interaction to 709, while only 639 genes were expressed in the S-interaction. By 2 dpi, the number of genes significantly decreased in the R-interaction while remaining relatively stable in the S-interaction. During late-stage infection at 5 dpi, the number of genes in the S-interaction rose to 888, representing approximately 99% of the total expressed genes detected. Comparatively, the number of genes expressed in the R-interaction decreased dramatically to 234. The total number of expressed genes has similar distributions to the percentage of mapped reads (Fig. 1). This is likely related to the power of detection at each time point in both the resistant and susceptible hosts.

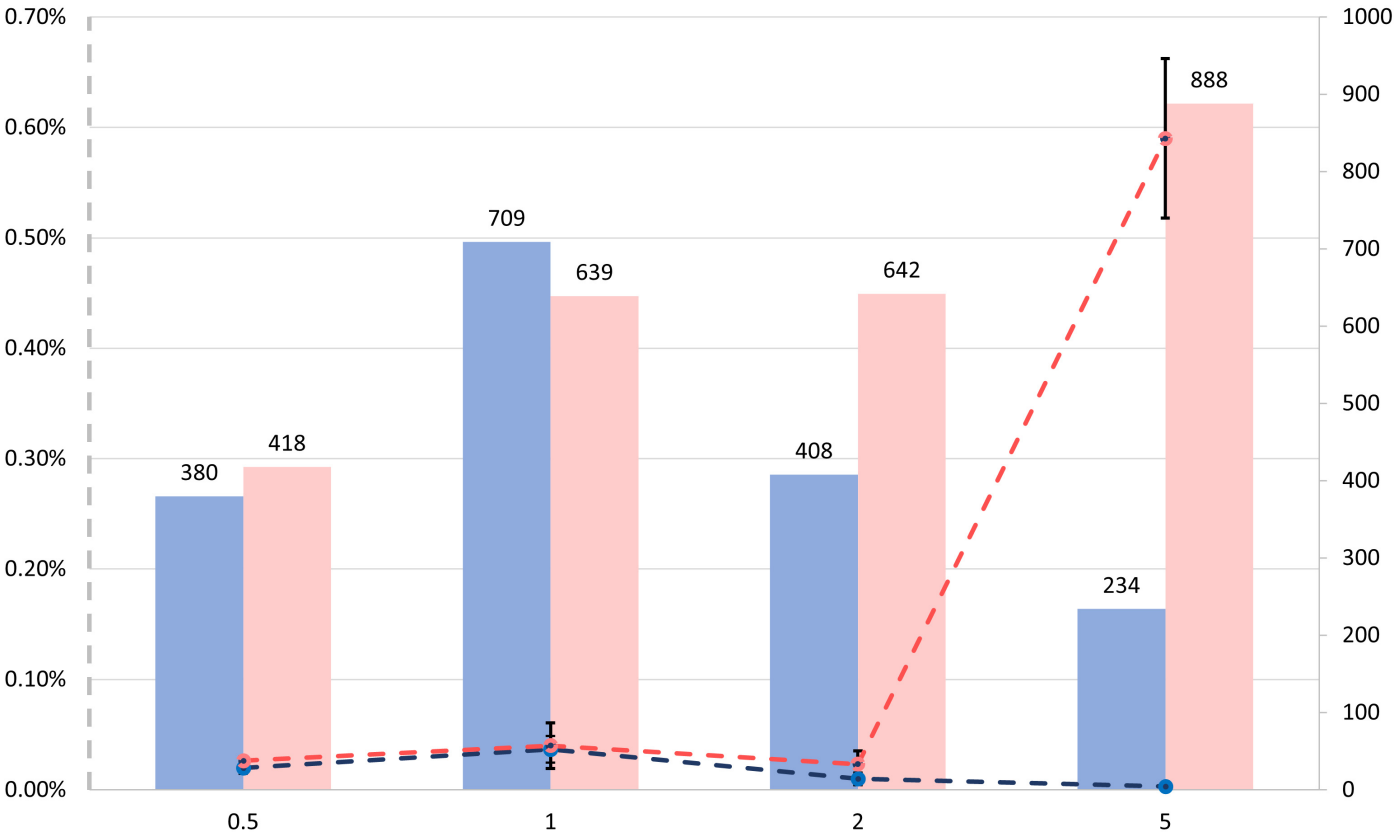

Fig. 1. The mapping statistics and the number of total expressed *Austropuccinia psidii* genes over the time series. Lines represent the percentage of mapped reads (primary *y*-axis) in the resistant (blue) and the susceptible (pink) interactions, error bars represent the standard error of the mean. The bars represent the total number of expressed genes (secondary *y*-axis) in the resistant (blue) and susceptible (pink) interactions. A total of 890 expressed genes were identified through RNA-seq analysis. The *x*-axis represents the time in days postinoculation.

Of the top 10 most highly expressed *A. psidii* genes, seven were common between the R- and S-interactions (Table 1; Supplementary Tables S2 and S3, respectively). Three of these genes are among the candidate effectors defined by Tobias et al. (2021). Moreover, five of these genes are among the list of DEGs at 5 dpi. Unfortunately, these genes had no successful annotations. It is imperative to determine the identity of these genes and the role they play during the interaction, as it may shed light on the pathogenicity and virulence of *A. psidii*. This is particularly true of the genes uniquely highly expressed in the S-interaction. Similarly, when investigating the top 100 most highly expressed genes, comparisons between the R- and S-interactions revealed 78 genes in common between interactions and 22 genes unique to either the R- or S-interaction.

When analyzing the total expressed genes using KEGG, 529 genes (approximately 59%) had successful annotations. The functional categories included genetic information processing (approximately 47%), carbohydrate metabolism (approximately 8%), cellular processes (approximately 6%), and energy metabolism (approximately 5%). KEGG enrichment revealed involvement of 2-oxocarboxylic acid metabolism, biosynthesis of amino acids, and glyoxylate and dicarboxylate metabolism among others (Supplementary Table S4).

Differentially expressed *A. psidii* genes

Differential gene expression analysis was performed to determine the differences in gene expression between the R- and S-interactions. *A. psidii* DEGs were considered up-regulated when expression was greater in the S-interaction compared with the R-interaction. Since there were only 890 confidently expressed *A. psidii* genes, there were very few DEGs. No DEGs were identified at 12 hpi and 2 dpi. At 1 dpi, *APSI_H004.3230* was significantly differentially expressed (DE) between the R- and S-interactions, with expression lower in the S-interaction ($\log_2$ (fold change) = –7.2). This gene did not have successful hits when functionally annotated, so putative functions are unknown. At 5 dpi, 11 genes were up-regulated with expression greater in the S-interaction, and 15 genes were down-regulated with expression lower in the S-interaction. Supplementary Table S5 shows the annotations of the 26 DEGs at 5 dpi.

GO enrichment analysis

GO enrichment analyses were performed to identify putative pathways involved in the interactions between *E. grandis* and *A. psidii*. There were no significantly overrepresented terms upon GO enrichment when analyzing the DE dataset. This is expected because of the small number of DEGs. When analyzing the total expressed gene space, 188 over-represented GO BP terms were identified across the R- and S-interactions over the time series (Fig. 2; Supplementary Table S6). These terms were predominantly associated with cellular processes, including terms such as translation, cellular protein metabolic process, and cellular biosynthetic process. These processes were shared among both the R- and S-interactions over time. Terms that were unique to the S-interaction included energy processes such as ATP synthesis, energy coupled proton transport, and mitochondrial ATP synthesis. Additionally, oxoacid metabolic processes and organic acid metabolic processes were also unique to the S-interaction. Terms unique to the R-interaction included glyoxylate cycle and metabolic process, dicarboxylic acid biosynthesis, and cellular aldehyde metabolic process.

Twenty-three overrepresented MF terms were identified across the R- and S-interactions. Terms unique to the S-interaction included malate dehydrogenase activity and saccharopine dehydrogenase activity, and terms involved in transcription were unique to the R-interaction (Supplementary Fig. S1). When investigating the CC category, 77 overrepresented terms were identified. Terms involving cellular processes were overrepresented, including transcription and translation (Supplementary Fig. S2).

A. psidii pathogenicity and virulence factors

The 890 confidently expressed myrtle rust genes aligned using the PHI database v4.2 (Urban et al. 2020). Genes with hits greater than 60% identity to the subject query, and those implicated in virulence and pathogenicity were retained for further analysis. The R-interaction had 24 genes with successful hits (Table 2; Supplementary Table S7), whereas the S-interaction had 32 genes with successful hits to the subject query (Table 2). Hits unique to the S-interaction included a gene involved in cAMP signaling (*Gib2*, *APSI_P008.17130, APSI_H002.12341*) and a gene encoding a putative pyridoxal 5′-phosphate synthase subunit (*PdxS*, *APSI_P009.17505*). Additionally, while the R- and S-interactions shared common hits, the S-interaction had expression of more orthologs of certain genes. These included expression of an additional *cyclophilin* (*CPA1*, *APSI_P005.10514*), *tubulin alpha-1 chain* (*TUB1*, *APSI_H010.14180*), *conserved actin protein* (*ActA*, *APSI_H003.4114*), *hypothetical protein* (*MGG_00383, APSI_H021.3806*), and a *beta2-tubulin* housekeeping gene (*APSI_H018.10108*). Hits shared between resistant and susceptible interactions included *heat shock proteins* (*HSPs*), a transcription factor gene identified in *Magnaporthe oryzae*, and a gene encoding *3-isopropylmalate dehydratase* (Table 2).

Analysis of the candidate effector proteins identified by Tobias et al. (2021) revealed a total of 43 expressed genes in the present study (Fig. 3A; Supplementary Table S8). The S-interaction had seven uniquely expressed candidate effectors over the course of infection, two at 2 dpi and five at 5 dpi (Supplementary Table S8). The expression of these genes was not observed in the R-interaction. To investigate putative virulence and pathogenicity of these candidates, the protein sequences were subjected to a BLASTp on the NCBI nonredundant database. In total, 17 of the 43 expressed genes had successful hits to proteins from other organisms, predominantly rust fungi. Many of these hits corresponded with hypothetical or

TABLE 1. Expressed *Austropuccinia psidii* pathogen–host interactions database (PHI)-annotated genes in the R-interaction with percentage identity greater than 60% and implications in pathogenicity and virulence

Gene	FPKM[a]		Description	Differential expression[b]	Candidate effector[c]
	Resistant	Susceptible			
APSI_H016.15346	114,834.2	63,263.2	–	Down	Yes
APSI_P008.17159	42,222.1	42,296.8	–	–	No
APSI_P015.13113	35,201.5	38,433.9	–	–	Yes
APSI_P016.16372	42,274.5	68,001.6	–	Up	Yes
APSI_P016.16375	40,218.8	57,525.0	–	Up	No
APSI_P017.12412	43,208.9	35,281.8	–	Down	No
APSI_P017.12428	29,575.3	25,499.5	–	Down	No

[a] Average fragment per kilobase million across the time series.
[b] Significant differential expression at 5 days postinoculation during colonization of susceptible relative to resistant *Eucalyptus grandis*.
[c] Candidate effectors based on the parameters defined by Tobias et al. (2021).

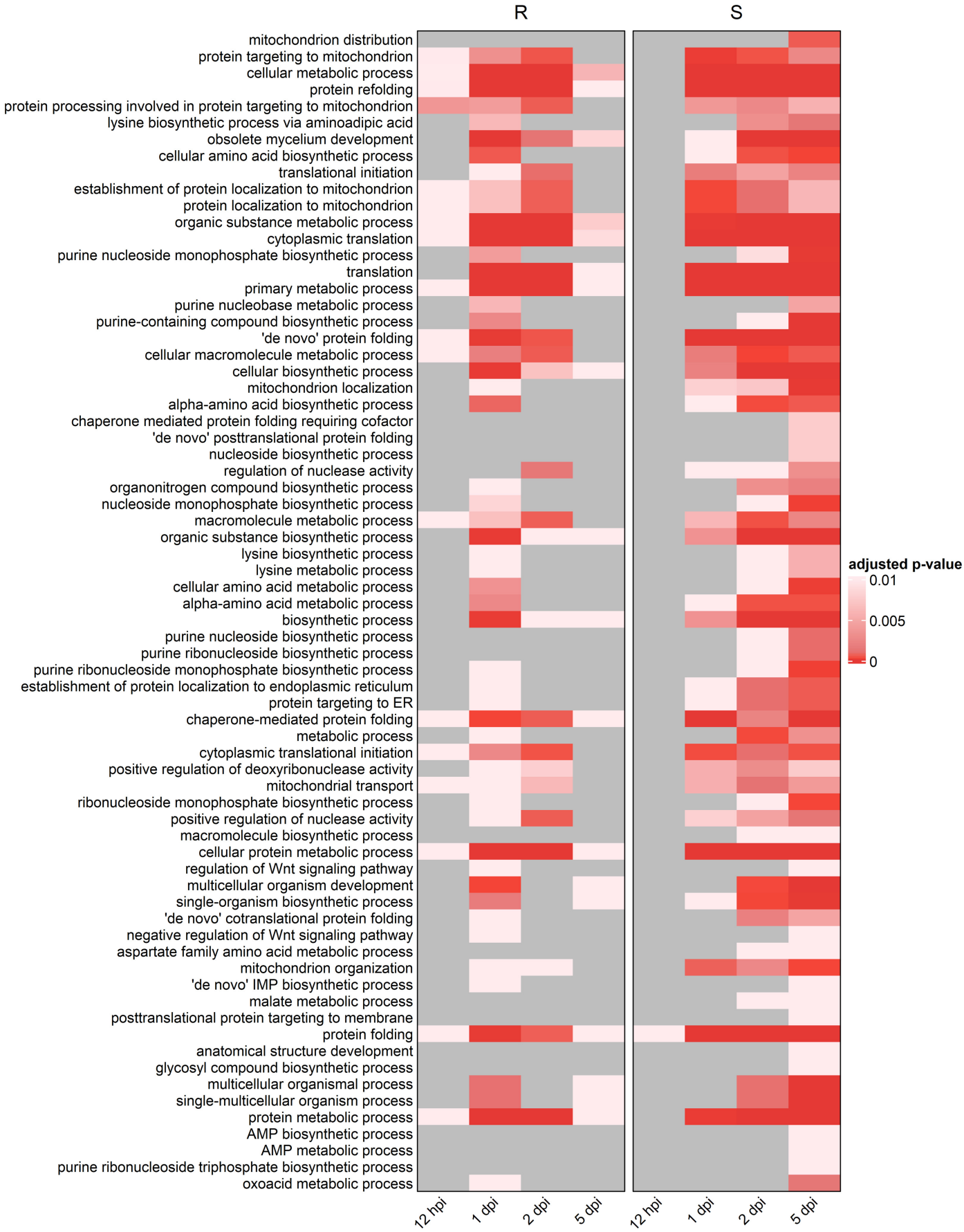

Fig. 2. Overrepresented gene ontologies (GO) in the biological processes (BP) category of total expressed *Austropuccinia psidii* genes in both the R- and S-interactions over the time series, where the color scale represents the false discovery rate (FDR) adjusted *P* value and gray represents absence of the term. GO analysis identified 188 overrepresented BP terms, and the heatmap represents the top 70 terms in relation to the lowest FDR value. R = resistant interaction; S = susceptible interaction; hpi = hours postinoculation; and dpi = days postinoculation.

uncharacterized proteins (Supplementary Table S9). Interestingly, five hits corresponded with informative hits (Table 3). A *small subunit ribosomal protein S10e* (*APSI_H017.8250*), a *rust transferred protein 1* (*RTP1*, *APSI_P008.18155*), and a *non-catalytic module family protein* (*APSI_H007.8820*) were uniquely expressed in the S-interaction. A *small subunit ribosomal protein S10e* (*APSI_P005.11212*) and a *hydrolase 76 protein* (*APSI_P004.3557*) were expressed in both interactions. The expression of these genes in the R- and S-interactions across the time series is represented by Figure 3B.

Comparisons of *A. psidii* transcriptome and proteome

To gain a deeper understanding of the key mechanisms governing the interaction between *A. psidii* and its hosts, the proteome results obtained by Quecine et al. (2016) were compared with the RNA-seq results obtained in the present study. There were 200 active and 140 obsolete entries (approximately 59%) for the proteins identified by Quecine et al. (2016) when retrieving protein sequences from UniProtKB/Swiss. This may be the result of improvements in the genomes of the organisms, making some entries obsolete or redundant. CRB BLAST results revealed 387 predicted *A. psidii* hits that are the most putative representatives of the proteins identified in the proteome study (Supplementary Table S10). From this, 82 genes were expressed in our transcriptome study (Table 4; Supplementary Table S11). These included *HSPs* that were either uniquely expressed in susceptible *P. guajava* or in greater abundance in *P. guajava* relative to resistant *E. grandis* (Quecine et al. 2016). There was greater expression of these *HSPs* in the R-interaction at 1 dpi, with expression in the S-interaction greater at 5 dpi. Other genes identified included those encoding for calnexin, enolase, pyruvate kinase, spermidine synthase, and tubulin beta chain proteins. Many *hypothetical protein* genes were identified within our dataset, with these uniquely abundant in *P. guajava* or *E. grandis* (Table 4).

Discussion

There have been limited studies on molecular genetics underlying the pathogen molecular dialogue with the host plant because of the obligate biotrophic nature of rust fungi. With improving next generation sequencing, omics studies have facilitated the study of these complex organisms, highlighting candidate pathogenicity genes that can be studied using heterologous systems (Bakkeren and Szabo 2020). This has broadened our understanding of rust disease and aided in development of efficient control strategies.

TABLE 2. Expressed *Austropuccinia psidii* pathogen–host interactions database (PHI)-annotated genes in the R- and S-interactions with percentage identity greater than 60% and implications in pathogenicity and virulence[a]

Query identity	Interaction	PHI base gene description	Identity (%)	Mutant phenotype
APSI_H008.9528	R + S	Cyclophillin	68	0
APSI_H009.11612	R + S	Ubiquitous chaperone, heat shock protein 90	64	0
APSI_H010.13601	R + S	Regulators of G-protein (GTP-binding protein) signaling (RGS) proteins/homocitrate synthase	64	0
APSI_H010.13652	R + S	Tubulin alpha-1 chain	78	1; 2
APSI_H010.13828	R + S	Glycogen synthase kinase, central signal regulator involved in the stress-responsive mechanism	69	1
APSI_H012.10735	R + S	Serine/threonine kinase	80	1
APSI_P001.5636	R + S	Heat shock protein	68	1
APSI_P001.5642	R + S	Heat shock protein	68	1
APSI_P001.5837	R + S	Uncharacterized protein	70	0
APSI_P001.6093	R + S	Calcium permease	61	0
APSI_P001.6880	R + S	Hypothetical protein	74	0
APSI_P002.14583	R + S	Regulators of G-protein (GTP-binding protein) signaling (RGS) proteins/homocitrate synthase	68	0
APSI_P002.15004	R + S	Glycogen synthase kinase	70	0; 1
APSI_P002.15358	R + S	Tubulin alpha-1 chain	74	1; 2
APSI_P003.1647	R + S	Cytochrome C peroxidase precursor	63	0
APSI_P003.2172	R + S	3-Isopropylmalate dehydratase	62	1
APSI_P011.231	R + S	Acetolactate synthase	65	1
APSI_P013.4275	R + S	Ubiquitous chaperone, heat shock protein 90	70	0
APSI_P014.1429	R + S	Transcription factor	62	1
APSI_P015.13025	R + S	Mitochondrial elongation factor Tu	63	0
APSI_P015.13172	R + S	Pyruvate kinase	61	0; 1
APSI_P017.12437	R + S	Conserved actin protein	90	0
APSI_P018.7518	R + S	Beta2-tubulin housekeeping gene	85	0
APSI_P020.4950	R + S	Bifunctional enzyme adenylosuccinate (ADS) lyase	77	0
APSI_H003.4114	S	Conserved actin protein	81	0
APSI_H018.10108	S	Beta2-tubulin housekeeping gene	85	0
APSI_P005.10514	S	Cyclophillin	68	0
APSI_P008.17130	S	Scaffolding protein promoting cAMP signaling	80	0
APSI_H002.12341	S	Scaffolding protein promoting cAMP signaling	80	0
APSI_H021.3806	S	Hypothetical protein	70	0
APSI_P009.17505	S	Pyridoxal 5′-phosphate synthase subunit PdxS	67	0
APSI_H010.14180	S	Tubulin alpha-1 chain	76	1; 2

[a] 0 = reduced virulence; 1 = loss of pathogenicity; 2 = lethal; R = genes unique to resistant interaction; S = genes unique to susceptible interaction; and R + S = genes expressed in both resistant and susceptible interactions.

TABLE 3. Informative protein BLAST results for the expressed candidate *Austropuccinia psidii* effectors in R- and S-interactions identified on the nonredundant NCBI database[a]

Candidate effector	Interaction	Accession	Identity (%)	Description	E-value
APSI_P005.11212	R + S	KNZ48236.1	81.5	Small subunit ribosomal protein S10e	3.55e–82
APSI_P004.3557	R + S	KAA1090934.1	75.9	Hydrolase 76 protein	7.44e–136
APSI_H017.8250	R + S	KNZ48236.1	82.2	Small subunit ribosomal protein S10e	5.49e–83
APSI_P009.18155	S	AFI13823.1	43.8	Rust transferred protein 1	2.13e–50
APSI_H007.8820	S	XP_007403659.1	38.7	Noncatalytic module family EXPN	1.23e–38

[a] R = genes unique to resistant interaction; S = genes unique to susceptible interaction; and R + S = genes expressed in both resistant and susceptible interactions.

TABLE 4. Comparison of *Austropuccinia psidii* genes differentially expressed (in susceptible relative to resistant *Eucalyptus grandis*) with differential protein abundance (in susceptible guava relative to resistant *E. grandis*) from Quecine et al. (2016)

Gene ID	Description	Log ratio (ApG/ApE)[a]	Log fold change (SI/RI)[b]			
			12 hpi	1 dpi	2 dpi	5 dpi
APSI_H002.12538	–	–0.84	0.00	0.24	0.61	0.87
APSI_P002.14830	–	0.22	0.00	0.00	0.00	1.65
APSI_P015.13025	–	ApGuava	0.00	–3.09	0.19	0.70
APSI_P004.3474	3-Isopropylmalate dehydrogenase	0.81	0.49	–0.71	–1.59	1.54
APSI_H009.11558	ATP synthase subunit alpha, mitochondrial	0.24	0.00	1.17	3.57	2.39
APSI_H005.1677	2-Isopropylmalate synthase	0.21	–3.42	–0.60	0.00	0.70
APSI_P002.15726	2-Methylcitrate dehydratase	0.3	2.80	–0.76	–0.41	0.85
APSI_P007.14326	3-Isopropylmalate dehydrogenase	0.81	–3.33	0.19	0.32	–0.72
APSI_H004.3682	40S ribosomal protein S7	–0.38	0.00	0.00	3.11	2.80
APSI_H001.6084	Acetyl-CoA carboxylase	ApEucalyptus	1.56	1.18	–0.32	–0.75
APSI_H003.4114	Actin	0.09	1.73	0.00	0.00	1.15
APSI_P017.12437	Actin	0.09	0.00	–2.32	1.43	2.06
APSI_H007.8988	Adenosylhomocysteinase	–0.01	–2.84	0.00	–0.32	0.98
APSI_H014.2045	Arabinitol dehydrogenase 1	0.18	0.00	0.00	0.20	1.22
APSI_H015.423	Arginyl-tRNA synthetase	0.11	0.00	0.59	0.00	0.44
APSI_H004.3499	Aspartate aminotransferase, mitochondrial	0.31	0.00	2.45	2.38	1.00
APSI_P004.2874	Aspartate aminotransferase, mitochondrial	0.31	–4.63	–4.06	0.09	2.46
APSI_P011.364	ATP synthase subunit beta, mitochondrial	0.14	0.94	–1.98	0.08	2.33
APSI_H014.2180	Calnexin	–0.4	0.37	–2.34	0.00	0.86
APSI_P005.10461	Calnexin	–0.4	–0.76	–1.37	–0.49	2.34
APSI_P005.10288	Chlorophyll synthesis pathway protein	0.18	0.37	–1.44	0.00	0.74
APSI_P016.16045	Elongation factor 2	0	–1.55	–1.17	3.01	2.74
APSI_P016.16081	Elongation factor 2	0	0.00	–1.71	1.45	2.69
APSI_H008.9525	Enolase	0.21	0.00	2.44	0.00	0.72
APSI_P005.10519	Enolase	0.21	0.00	–2.32	1.20	1.47
APSI_P010.11580	Eukaryotic translation initiation factor 3 subunit F	0.13	–1.64	0.41	0.06	–0.35
APSI_H014.2368	Fatty acid synthase subunit beta	ApEucalyptus	0.00	0.00	0.00	0.00
APSI_P005.10846	Fatty acid synthase subunit beta	ApEucalyptus	–0.59	–1.69	–0.82	0.36
APSI_H003.4176	Glucose-regulated protein	0.08	0.00	1.86	0.00	0.42
APSI_P017.12534	Glucose-regulated protein	0.08	0.00	0.18	1.44	0.57
APSI_P008.16892	Glutamate dehydrogenase	0.14	0.00	–1.46	3.52	0.59
APSI_P010.11420	Heat shock 70kda protein 4	0.49	0.00	–3.15	2.06	2.69
APSI_P010.11427	Heat shock 70kda protein 4	0.49	0.56	–2.92	1.67	3.11
APSI_P013.4275	Heat shock protein 83	0.1	–1.53	–1.10	1.40	1.15
APSI_H022.14	Heat shock protein HSS1	0.08	–4.43	–0.32	4.02	2.33
APSI_P009.17506	Heat shock protein HSS1	0.08	–0.15	–0.54	1.38	2.63
APSI_P001.5636	Heat shock protein SSB	0.17	–3.65	0.01	1.50	3.38
APSI_P001.5642	Heat shock protein SSB	0.17	–1.73	–0.02	1.18	3.37
APSI_H009.11612	Heat shock protein 90	0.1	–1.37	0.23	2.27	1.73
APSI_H001.6204	Hsp70-like protein	0.3	0.00	3.92	1.51	2.42
APSI_P002.14610	Hsp70-like protein	0.3	0.00	0.34	2.32	–0.08
APSI_P008.17020	Hypothetical protein	ApEucalyptus	1.16	–2.20	–0.03	0.54
APSI_H016.15678	Hypothetical protein	ApGuava	0.00	0.00	1.54	0.66
APSI_H001.6960	Hypothetical protein	0.43	0.00	1.86	2.17	0.10
APSI_P014.1140	Hypothetical protein	0.35	1.87	2.30	1.69	1.76
APSI_H003.4994	Hypothetical protein	–0.09	0.00	0.00	1.43	1.98
APSI_P014.1093	Hypothetical protein	–0.09	0.00	1.24	0.97	2.08
APSI_P001.5930	Hypothetical protein	ApEucalyptus	2.73	3.47	1.44	0.18
APSI_H018.10185	Hypothetical protein	ApGuava	1.96	0.00	–1.14	0.01
APSI_H016.15562	Hypothetical protein	0.36	0.00	–0.24	0.00	2.01
APSI_P010.11387	Hypothetical protein	–0.17	–0.38	0.88	–1.28	–0.94
APSI_H006.15165	Hypothetical protein	–0.05	–3.58	1.01	2.07	0.83
APSI_P009.17824	Hypothetical protein	ApGuava	0.00	–1.98	2.17	1.28
APSI_P006.9484	Hypothetical protein	ApGuava	0.00	0.00	0.92	1.06
APSI_P003.1597	Hypothetical protein	ApGuava	0.00	0.04	–1.04	0.56
APSI_P011.239	Hypothetical protein	–0.21	2.28	–1.36	–4.68	–0.79
APSI_P011.268	Hypothetical protein	0.53	3.14	–3.06	1.95	0.62
APSI_P019.8310	Hypothetical protein	0.43	0.00	0.00	1.54	0.10
APSI_P011.233	Hypothetical protein	ApGuava	0.00	0.05	2.88	1.73
APSI_P016.16382	Hypothetical protein	0.16	–0.51	–0.92	0.52	2.77
APSI_H017.8116	Hypothetical protein	0.03	0.00	–0.60	0.00	0.50
APSI_H017.8250	Hypothetical protein	ApGuava	0.00	0.00	0.00	1.22
APSI_P012.9011	Kinesin family member C1	0.06	1.45	1.05	1.40	2.81
APSI_H001.6292	Malate dehydrogenase, NAD-dependent	0.56	0.00	–1.26	2.08	1.75
APSI_P003.1614	Malate dehydrogenase, NAD-dependent	0.56	0.00	1.40	–0.49	1.72
APSI_H013.5798	Minichromosome maintenance protein 4	ApGuava	1.17	–1.35	1.58	–0.08
APSI_P010.11499	Minichromosome maintenance protein 6	0	–2.30	2.95	1.20	–0.37
APSI_P001.6720	Polyubiquitin-A	ApEucalyptus	–0.31	–0.22	–0.64	0.37

(*Continued on next page*)

[a] Log ratio of ApGuava relative to ApEucalyptus (Quecine et al. 2016).

[b] Log fold change of susceptible relative to resistant *Eucalyptus grandis*; ApG = *A. psidii* guava; ApE = *A. psidii E. grandis*; SI = S-interaction; and RI = R-interaction.

TABLE 4. (*Continued from previous page*)

Gene ID	Description	Log ratio (ApG/ApE)[a]	Log fold change (SI/RI)[b]			
			12 hpi	1 dpi	2 dpi	5 dpi
APSI_P017.12651	Polyubiquitin-A	ApEucalyptus	0.00	–1.44	0.00	1.41
APSI_H009.11705	Protein transporter SEC23	0.06	0.00	1.24	1.44	0.30
APSI_P013.4176	Protein transporter SEC23	0.06	0.00	2.49	0.91	0.40
APSI_H016.15523	Putative histone H9	ApEucalyptus	0.00	–3.77	1.43	0.39
APSI_P015.13172	Pyruvate kinase	ApGuava	–0.59	0.00	0.00	–0.29
APSI_P005.10979	RuvB-like helicase 1	ApGuava	0.37	–3.25	1.45	1.05
APSI_P016.16384	Secretory pathway GDP dissociation inhibitor 1	0.68	0.00	0.29	0.00	0.39
APSI_P018.7791	Spermidine synthase	ApGuava	0.00	1.07	0.31	0.29
APSI_P007.14016	T-complex protein 1 subunit alpha	–0.12	0.00	–1.62	0.00	–0.04
APSI_H006.15105	Translation initiation factor eIF-3	–0.11	0.00	0.00	0.00	0.28
APSI_H018.10108	Tubulin beta chain	0.34	0.00	0.00	0.00	0.72
APSI_P018.7518	Tubulin beta chain	0.34	0.00	–1.09	0.00	0.38
APSI_P002.15126	Uncharacterized protein	ApGuava	0.00	1.21	2.57	0.65
APSI_P007.13634	Vacuolar protein 8	ApGuava	–1.52	–0.54	–0.72	2.30

The present study investigated the molecular responses of the pandemic biotype of *A. psidii* in resistant and susceptible *E. grandis*. This was achieved by pooling 14 highly heterozygous seedlings in three replicates per phenotype per time point. Despite the high heterozygosity of host material within and between samples, host responses were previously observed to be consistent between biological replicates (Swanepoel et al. 2021) and similarly, pathogen expression showed consistency between hosts over time. However, key differences between hosts were observed, including unique expression of candidate effectors in susceptible hosts as well as pathogenicity and virulence factors and pathways potentially contributing to disease. The results of this study are similar to those of Quecine et al. (2016), revealing that *A. psidii* might employ similar mechanisms to elicit host disease in different plant species.

Over the course of infection, the number of reads mapping to the pathogen genome decreased in the R-interaction. This suggests that over the course of infection, the R-interaction successfully suppresses the growth and development of the pathogen, thereby reducing the number of pathogen transcripts observed in the analysis. The number of reads mapping to the reference genome in S-interaction significantly increases over the course of infection, suggesting that the S-interaction does not mount an effective defense response to prevent the proliferation of the pathogen. This is observed in the interaction between *A. psidii* and *M. quinquenervia*, where the number of reads mapping to the resistant hosts was 0% compared with 2% in the susceptible hosts, suggesting only susceptible hosts facilitate the growth of the pathogen at 5 dpi (Hsieh et al. 2018). This is observed in the present study, where the greatest number of expressed genes in the analysis were identified in the S-interaction at 5 dpi ($n = 888$). These results are further supported by Tobias et al. (2018) in which resistant hosts actively respond to *A. psidii* infection, while susceptible hosts lack a sufficient, coordinated response, potentially contributing to the number of transcripts observed. This corroborates the results obtained in our previous studies on *E. grandis* responses to *A. psidii* (Swanepoel et al. 2021), where the infection on susceptible leaves presented as severe pustules of urediniodspores progressing over the course of infection.

Shared virulence and pathogenicity factors

In the present study, analysis of expressed candidate effectors revealed a *family 76 hydrolase protein* gene expressed in both the R- and S-interactions across the time series. Furthermore, a putative *family 61 glycoside hydrolase protein* was DE at 5 dpi, with expression significantly greater in the R-interaction compared with the S-interaction. These are classes of CWDEs that are employed by pathogens to degrade preformed barriers. Hydrolase proteins are known to contribute to the degradation of plant cell walls in other rust fungi (Cooper et al. 2016; Wu et al. 2019). Greater expression of these genes in the R-interaction is unexpected. It is possible that the pathogen is overexpressing these CWDE in resistant hosts to compensate for the effective preformed barriers that are preventing pathogen entry into the host plant (dos Santos et al. 2019). In the interaction with *A. psidii* and *E. grandis,* it was found that callose deposition was enriched across the time series in resistant *E. grandis,* while this was poorly coordinated in the susceptible hosts, only enriched at 5 dpi (Swanepoel et al. 2021). Thus, entry into the plant cells could occur with relative ease and more rapidly in susceptible hosts, as preformed barriers may not be adequate to prevent pathogen entry. Tobias et al. (2018) supports this, where infected resistant *S. luehmannii* was found to have greater expression of a secondary cell wall synthesis gene that encodes beta-1,4-xylosyltransferase compared with susceptible hosts. This suggests that preformed barriers are more prominent in resistant hosts. These results highlight a prominent area for future work.

Among the genes found in the interaction were numerous *HSPs*. HSPs are known to be involved in chaperoning the folding of proteins, but they also function to protect the cell from stress, including heat stress, fluctuations in pH, and oxidative stress (Pandey et al. 2018; Tiwari et al. 2015). Two *HSPs 90* (*APSI_P013.4275, APSI_H009.11612*) were identified as potential virulence factors in both the R- and S-interactions when compared with PHI-base. HSP90 is involved in the complex protein folding processes and is vital to the functioning of the organism (Nathan et al. 1997). Previous studies on rust fungi virulence and pathogenicity factors have identified a plethora of HSPs enriched in susceptible hosts, suggesting that these proteins play crucial roles in facilitating plant disease (Cooper et al. 2016; Quecine et al. 2016). Quecine et al. (2016) identified various pathogen-derived HSPs during the interactions with *A. psidii,* with more HSPs identified in susceptible *P. guajava* than in resistant *E. grandis*. This is further supported by Song et al. (2011), where numerous HSPs were isolated from the haustoria of *Puccinia triticina,* a wheat leaf rust fungus. The expression of *HSPs* in this study suggests a significant role of these proteins in the interaction between *A. psidii* and *E. grandis*.

Amino acid biosynthesis and metabolism pathways were significantly enriched in both the R- and S-interactions. The gene encoding the enzyme 3-isopropylmalate dehydratase, involved in the biosynthesis of leucine, was identified as a putative pathogenicity factor when compared with the PHI-base in both interactions (Table 2). Moreover, one of these proteins was identified in the urediniospores of *P. guajava* and *E. grandis*, where abundance was greater in susceptible *P. guajava* than in resistant *E. grandis* (log ratio = 0.81, Table 4; Supplementary Table S11; Quecine et al. 2016). This implicates this enzyme in the disease process of *A. psidii* and tags it as an important pathway for disease control strategies.

Virulence and pathogenicity factors uniquely expressed in susceptible hosts

PdxS was found to contribute to viability, stress tolerance, and virulence of the gram-negative bacterial pathogen, *Actinobacillus pleuopneumoniae,* which causes pleuropneumonia respiratory disease (Xie et al. 2017). PdxS catalyzes the production of pyridoxal 5′-phosphate (PLP), a biochemically active form of vitamin B6 (Eliot and Kirsch 2004). *PdxS* mutants exhibited abnormal morphology, with craters on their surfaces, suggesting that adequate production of PLP by PdxS is required for normal cell morphology (Xie et al. 2017). PLP is a cofactor for phosphorylation, playing a key role in many physiological processes, including amino acid biosynthesis and metabolism. In a study conducted by Song et al. (2011) on *P. triticina*, a Pdx1 protein was isolated from the haustoria during interactions with wheat. Moreover, a pyridoxine biosynthesis protein was more abundant in susceptible *P. guajava* than resistant *Eucalyptus* when investigating the proteome of *A. psidii*-infected hosts (Quecine et al. 2016).

Rust transferred protein 1 may manipulate the reactive oxygen species production

Five expressed *A. psidii* candidate effector genes had successful annotations when subjected to BLAST analysis (Table 3). A *rust transferred protein* (*RTP1*) was identified in the S-interaction at 5 dpi, with expression of this gene not detected in the R-interaction. This protein, initially identified in *Uromyces fabae*, was found to localize in the extra-haustoria matrix during early stages of infection as well as inside the host cell cytoplasm as the disease progresses and the haustoria matures. This suggests RTP1 plays a crucial role in maintaining the biotrophic lifestyle with host plants (Kemen et al. 2005, 2013). It was found that as the haustoria matures over the course of infection, high concentrations of RTP1p can be found within the host cytoplasm (Kemen et al. 2013). As a result, cyclosis of host nucleus and chloroplasts is inhibited, with the authors suggesting this cessation is the result of accumulation of RTP1p (Kemen et al. 2013).

Oxalic acid may manipulate host oxidative and phytohormone pathways

In the present study, genes involved in malate dehydrogenase, oxoacid metabolism, and malate metabolism were identified (Supplementary Fig. S1; Fig. 2). Malate dehydrogenase is an enzyme that catalyzes the reaction of malate to oxaloacetate, a precursor molecule for oxalic acid production. The accumulation of oxalic acid produces an acidic environment within the host plant to facilitate crucial fungal mechanisms of infection, which includes the secretion of virulence factors (Lovat and Donnelly 2019). Oxalic acid is known to reduce plant oxidative burst responses and produce an acidic environment in the host cells to facilitate disease in host plants (Cessna et al. 2000; Laurent et al. 1993). In the interaction between *Castanea* spp. and the chestnut blight pathogen *Cryphonectria parasitica*, oxalate (oxalic acid) is produced by the pathogen, reducing the host cellular pH to promote the functioning of crucial fungal enzymes that manipulate oxidative burst (Lovat and Donnelly 2019). A previous study investigating *E. grandis* responses to *A. psidii* found significant involvement of the oxidative burst response in defense response (Swanepoel et al. 2021). The plant-type HR was prominent in resistant hosts at 2 and 5 dpi, whereas susceptible hosts only responded with HR at 5 dpi. This suggests that despite both hosts regulating and mounting respiratory burst responses, the susceptible hosts lacked the ability to convert these into HR. This may be because of the involvement of the pathogen-secreted virulence factor such as malate dehydrogenase and oxalic acid.

In the same study, the authors found the putative involvement of phytohormones in the host responses to *A. psidii* (Swanepoel et al. 2021). This included SA, jasmonic acid (JA), ethylene (ET), and abscisic acid (ABA) enriched in both the R- and S-interactions, as well as brassinosteroids (BR) enriched only in the R-interaction. Applications of oxalic acid to *Brassica napus* L. has been shown to affect phytohormone signaling within the plant (Liang et al. 2009). Proteins associated with phytohormone pathways including JA and ET were increased following applications of oxalic acid. Despite

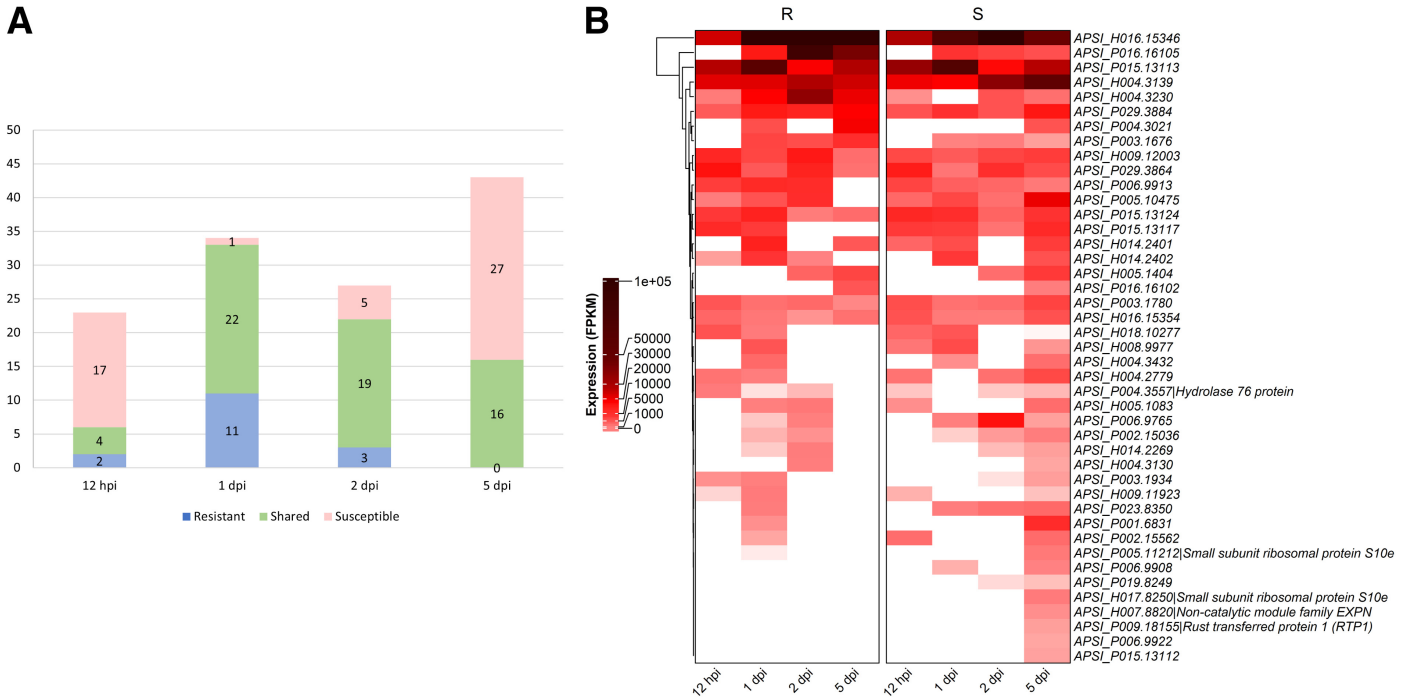

Fig. 3. The expression of *Austropuccinia psidii* effector genes. **A,** The number of expressed *A. psidii* candidate effectors. Blue represents the genes expressed in the R-interaction, green represents expressed genes between the R- and S-interactions, and pink represents effector genes expressed in the S-interaction. **B,** The expression of patterns of *A. psidii* effectors genes in both the resistant and susceptible *Eucalyptus grandis* interactions over the time series. Genes with known annotations are labeled. The color gradient represents the expression values of a measure of fragment per kilobase million (FPKM) ranging from the minimum to maximum expression values, where white represents genes that are not expressed. hpi = hours postinoculation; dpi = days postinoculation; R = resistant interaction; and S = susceptible interaction.

the evidence suggesting that SA is not directly affected in the presence of oxalic acid, it was found that pathways mediated by the phytohormone were decreased (Liang et al. 2009). Therefore, we hypothesize that *A. psidii* may produce oxalic acid to manipulate the phytohormone crosstalk within susceptible *E. grandis*.

While comparisons between the proteome (Quecine et al. 2016) and the transcriptome of *A. psidii* provide valuable insights into the molecular mechanisms governing the interactions of *A. psidii* with its hosts, it is important to remember that the timing of collection of materials for analysis plays a role in the outcome of the results obtained. Furthermore, the study conducted on the proteome isolated urediniospores of *P. guajava* and *E. grandis*, whereas the present study isolated fungal RNA from whole leaf samples. Different infection structures and stages can affect the results obtained. Additionally, Quecine et al. (2016) considered the differences that exist between different species, whereas the present study aimed to determine the differences that exist within *E. grandis* provenances. Therefore, the results obtained in the comparisons need to be further validated to confirm how the proteins and genes found contribute to disease susceptibility.

Conclusions

The interaction between resistant and susceptible *E. grandis* and *A. psidii* share similarities, with the timing of infection crucial to the disease progression, highlighted by unique pathogen genes expressed solely in the S-interaction at 5 dpi. Several pathways were shown in this study, putatively contributing to the molecular dialogue with *E. grandis*. This is the first study to investigate the expression of *A. psidii* genes in planta over a time series. Through this, several candidate *A. psidii* genes and pathways have been identified for future functional studies that investigate their roles in the interaction with *E. grandi*s. This includes the uniquely expressed *RTP1* gene, various *HSP* genes, *CWDE* genes, as well as the putative involvement of oxalic acid in pathogenicity. In conclusion, this reveals genes and pathways that may be manipulated to control the devastating effects this pathogen has on native and introduced Myrtaceae species.

Literature Cited

Aime, M. C., McTaggart, A. R., Mondo, S. J., and Duplessis, S. 2017. Phylogenetics and phylogenomics of rust fungi. Adv. Genet. 100:267-307.

Aubry, S., Kelly, S., Kümpers, B. M. C., Smith-Unna, R. D., and Hibberd, J. M. 2014. Deep evolutionary comparison of gene expression identifies parallel recruitment of trans-factors in two independent origins of C4 photosynthesis. PLoS Genet. 10:e1004365.

Bakkeren, G., and Szabo, L. J. 2020. Progress on molecular genetics and manipulation of rust fungi. Phytopathology 110:532-543.

Beenken, L. 2017. *Austropuccinia*: A new genus name for the myrtle rust *Puccinia psidii* placed within the redefined family Sphaerophragmiaceae (Pucciniales). Phytotaxa 297:53-61.

Buchfink, B., Xie, C., and Huson, D. H. 2015. Fast and sensitive protein alignment using DIAMOND. Nat. Methods 12:59-60.

Carnegie, A. J., Lidbetter, J. R., Walker, J., Horwood, M. A., Tesoriero, L., Glen, M., and Priest, M. J. 2010. *Uredo rangelii*, a taxon in the guava rust complex, newly recorded on Myrtaceae in Australia. Australas. Plant Pathol. 39:463-466.

Cessna, S. G., Sear, V. E., Dickman, M. B., and Low, P. S. 2000. Oxalic acid, a pathogenicity factor for *Sclerotinia sclerotiorum*, suppresses the oxidative burst of the host plant. Plant Cell 12:2191-2199.

Cooper, B., Campbell, K. B., Beard, H. S., Garret, W. M., and Islam, N. 2016. Putative rust fungal effector proteins in infected bean and soybean leaves. Phytopathology 106:491-499.

Coutinho, T. A., Wingfield, M. J., Alfenas, A. C., and Crous, P. W. 1998. *Eucalyptus* rust: A disease with the potential for serious international implications. Plant Dis. 82:819-825.

Dobin, A., Davis, C. A., Schlesinger, F., Drenkow, J., Zaleski, C., Jha, S., Batut, P. B., Chaisson, M., and Gingeras, T. R. 2013. STAR: Ultrafast universal RNA-seq aligner. Bioinformatics 29:15-21.

dos Santos, I. B., Lopes, M. D. S., Bini, A. P., Tschoeke, B. A. P., Verssani, B. A. W., Figueredo, E. F., Cataldi, T. R., Marques, J. P. R., Silva, L. D., Labate, C. A., and Quecine, M. C. 2019. The *Eucalyptus* cuticular waxes contribute in preformed defense against *Austropuccinia psidii*. Front. Plant Sci. 9:1978.

du Plessis, E., Granados, G. M., Barnes, I., Ho, W. H., Alexander, B. J. R., Roux, J., and McTaggart, A. R. 2019. The pandemic strain of *Austropuccinia psidii* causes myrtle rust in New Zealand and Singapore. Australas. Plant Pathol. 48:253-256.

du Plessis, E., McTaggart, A. R., Granados, M. J., Wingfield, M. J., Roux, J., Ali, M. I. M., Pegg, G. S., Makinson, J., and Purcell, M. 2017. First report of myrtle rust caused by *Austropuccinia psidii* on *Rhodomyrtus tomentosa* (Myrtaceae) from Singapore. Plant Dis. 101:1676.

Edwards, R. J., Dong, C., Park, R. F., and Tobias, P. A. 2022. A phased chromosome-level genome and full mitochondrial sequence for the dikaryotic myrtle rust pathogen, *Austropuccinia psidii*. bioRxiv 2022.04.22.489119.

Eliot, A. C., and Kirsch, J. F. 2004. Pyridoxal phosphate enzymes: Mechanistic, structural, and evolutionary considerations. Annu. Rev. Biochem. 73: 383-415.

Giblin, F. 2013. Myrtle rust report: New Caledonia. Assessment of myrtle rust situation in New Caledonia. University of the Sunshine Coast Maroochydore, Queensland, Australia.

Glen, M., Alfenas, A. C., Zauza, E. A. V., Wingfield, M. J., and Mohammed, C. 2007. *Puccinia psidii*: A threat to the Australian environment and economy–A review. Australas. Plant Pathol. 36:1-16.

Goodstein, D. M., Shu, S., Howson, R., Neupane, R., Hayes, R. D., Fazo, J., Mitros, T., Dirks, Q., Hellsten, U., Putnam, N., and Rokhsar, D. S. 2011. Phytozome: A comparative platform for green plant genomics. Nucleic Acids Res. 40:D1178-D1186.

Grattapaglia, D., Vaillancourt, R. E., Shepard, M., Thumma, B. R., William, F., Külheim, C., Potts, B. M., and Myburg, A. A. 2012. Progress in Myrtaceae genetics and genomics: *Eucalyptus* as the pivotal genus. Tree Genet. Genomes 8:463-508.

Hart, A. J., Ginzburg, S., Xu, M., Fisher, C. R., Rahmatpur, N., Mitton, J. B., Paul, R., and Wegrzyn, J. L. 2019. EnTAP: Bringing faster and smarter functional annotation to non-model eukaryotic transcriptomes. Mol. Ecol. Resour. 20:591-604.

Hsieh, J.-F., Chuah, A., Patel, H. R., Sandu, K. S., Foley, W. J., and Külheim, C. 2018. Transcriptome profiling of *Melaleuca quinquenervia* challenged by myrtle rust reveals differences in defense responses among resistant individuals. Phytopathology 108:495-509.

Huerta-Cepas, J., Szklarczyk, D., Heller, D., Hernández-Plaza, A., Forslund, S. K., Cook, H., Mende, D. R., Letunic, I., Rattei, T., Jensen, L. J., von Mering, C., and Bork, P. 2019. eggnog 5.0: A hierarchical, functionally and phylogenetically annotated orthology resource based on 5090 organisms and 2502 viruses. Nucleic Acids Res. 47:D309-D314.

Jones, P., Binns, D., Chang, H.-F., Fraser, M., Li, W., McAnulla, C., McWilliam, H., Maslen, J., Mitchell, A., Nuka, G., Pesseat, S., Quinn, A. F., Sangrador-Vegas, A., Scheremetjew, M., Yong, S.-Y., Lopez, R., and Hunter, S. 2014. InterProScan 5: Genome-scale protein function classification. Bioinformatics 30:1236-1240.

Junghans, D. T., Alfenas, A. C., Brommonschenkel, S. H., Oda, S., Mello, E. J., and Grattapaglia, D. 2003a. Resistance to rust (*Puccinia psidii* Winter) in *Eucalyptus*: Mode of inheritance and mapping of a major gene with RAPD markers. Theor. Appl. Genet. 108:175-180.

Junghans, D. T., Alfenas, A. C., and Maffia, L. A. 2003b. Escala de notas para quantificação da ferrugem em *Eucalyptus*. Fitopatol. Bras. 28:184-188.

Kanehisa, M., Araki, M., Goto, S., Hattori, M., Hirakawa, M., Itoh, M., Katayama, T., Kawashima, S., Okuda, S., Tokimatsu, T., and Yamanishi, Y. 2008. KEGG for linking genomes to life and the environment. Nucleic Acid Res. 36:D480-D484.

Kawanishi, T., Uematsu, S., Kakishima, M., Kagiwada, S., Hamamoto, H., Horie, H., and Namba, S. 2009. First report of rust disease on ohia and the causal fungus, *Puccinia psidii,* in Japan. J. Gen. Plant. Pathol. 75:428-431.

Kemen, E., Kemen, A. C., Ehlers, A., Voegele, R. T., and Mendgen, K. 2013. A novel structural effector from rust fungi is capable of fibril formation. Plant J. 75:767-780.

Kemen, E., Kemen, A. C., Rafiqi, M., Hempel, U., Mendgen, K., Hahn, M., and Voegele, R. T. 2005. Identification of a protein from rust fungi transferred from haustoria into infected plant cells. Mol. Plant-Microbe. Interact. 18:1130-1139.

Laurent, L., Susan, R., Heinstein, P. F., and Low, P. S. 1993. Characterization of the oligogalacturonide-induced oxidative burst in cultured soybean (*Glycine max*) cells. Plant Physiol. 102:233-240.

Liang, Y., Strelkov, S. E., and Kav, N. N. V. 2009. Oxalic acid-mediated stress responses in *Brassica napus* L. Proteomics 9:3156-3173.

Lovat, C.-A., and Donnelly, D. J. 2019. Mechanisms and metabolomics of the host-pathogen interactions between chestnut (*Castanea species*) and chestnut blight (*Cryphonectria parasitica*). For. Pathol. 49:e12562.

Love, M. I., Huber, W., and Anders, S. 2014. Moderated estimation of fold change and dispersion for RNA-seq data with DESeq2. Genome Biol. 15: 550.

Madina, M. H., Rahman, M. S., Huang, X., Zhang, Y., Zheng, H., and Germain, H. 2020. A poplar rust effector protein associates with protein disulfide isomerase and enhances plant susceptibility. Biology 9:294.

Marlatt, R. B., and Kimbrough, J. W. 1979. *Puccinia psidii* on *Pimenta dioica* in south Florida. Plant Dis. Rep. 63:510-512.

McTaggart, A. R., Roux, J., Granados, G. M., Gafur, A., Tarrigan, M., Santhakumar, P., and Wingfield, M. J. 2016. Rust (*Puccinia psidii*) recorded in Indonesia poses a threat to forests and forestry in South-East Asia. Australas. Plant Pathol. 45:83-89.

Minchinton, E. J., Smith, D., Hamley, K., and Donald, C. 2014. Myrtle rust in Australia. Acta Hortic. 1055:89-90.

Myburg, A. A., Grattapaglia, D., Tuskan, G. A., Hellsten, U., Hayes, R. D., Grimwood, J., Jenkins, J., Lindquist, E., Tice, H., Bauer, D., Goodstein, D. M., Dubchak, I., Poliakov, A., Mizrachi, E., Kullan, A. R. K., Hussey, S. G., Pinard, D., van der Merwe, K., Singh, P., van Jaarsveld, I., Silva-Junior, O. B., Togawa, R. C., Pappas, M. R., Faria, D. A., Sansaloni, C. P., Petroli, C. D., Yang, C., Ranjan, P., Tschaplinski, T. J., Ye, C.-Y., Li, T., Sterck, L., Vanneste, K., Murat, F., Soler, M., Clemente, H. S., Saidi, N., Cassan-Wang, H., Dunand, C., Hefer, C. A., Bornberg-Bauer, E., Kersting, A. R., Vining, K., Amarasinghe, V., Ranik, M., Naithani, S., Elser, J., Boyd, A. E., Liston, A., Spatafora, J. Q., Dharmwardhana, P., Raja, R., Sullivan, C., Romanel, E., Alves-Ferreira, M., Külheim, C., Foley, W., Carocha, V., Paiva, J., Kudrna, D., Brommonschenkel, S. H., Pasquali, G., Byrne, M., Rigault, P., Tibbits, J., Spokevicius, A., Jones, R. C., Steane, D. A., Vaillancourt, R. E., Potts, B. M., Joubert, F., Barry, K., Pappas, G. J., Strauss, S. H., Jaiswal, P., Grima-Pettenati, J., Salse, J., Van de Peer, Y., Rokhsar, D. S., and Schmutz, J. 2014. The genome of *Eucalyptus grandis*. Nature 510:356-362.

Naidoo, R., Ferreira, L., Berger, D. K., Myburg, A. A., and Naidoo, S. 2013. The identification and differential expression of *Eucalyptus grandis* pathogenesis-related genes in response to salicylic acid and methyl jasmonate. Front. Plant Sci. 4:43.

Nathan, D. F., Vos, M. H., and Lindquist, S. 1997. *In vivo* functions of the *Saccharomyces cerevisiae* Hsp90 chaperone. Proc. Natl. Acad. Sci. 94:12949-12956.

Pandey, V., Singh, M., Pandey, D., and Kumar, S. 2018. Integrated proteomics, genomics, metabolomics approaches reveal oxalic acid as pathogenicity factor in *Tilletia indica* inciting Karnal bunt disease of wheat. Sci. Rep. 8:7826.

Pertea, M., Pertea, G. M., Antonescu, C. M., Chang, T.-C., Mendall, J. T., and Salzberg, S. L. 2015. StringTie enables improved reconstruction of a transcriptome from RNA-seq reads. Nat. Biotechnol. 33:290-295.

Petre, B., Joly, D. L., and Duplessis, S. 2014. Effector proteins of rust fungi. Front. Plant Sci. 5:416.

Quecine, M. C., Leite, T. F., Bini, A. P., Regiani, T., Franceschini, L. M., Budzinski, I. G. F., Marques, F. G., Labate, M. T. V., Guidetti-Gonzalez, S., Moon, D. H., and Labate, C. A. 2016. Label-free quantitative proteomic analysis of *Puccinia psidii* uredospores reveals differences of fungal populations infecting *Eucalyptus* and guava. PLoS One 11:e0145343.

R Core Team. 2018. R: A language and environment for statistical computing. R Foundation for Statistical Computing, Vienna, Austria.

Rayachhetry, M. B., Elliot, M. L., and Van, T. K. 1997. Natural epiphytotic of the rust *Puccinia psidii* on *Melaleuca quinquenervia* in Florida. Plant Dis. 81:831.

Roux, J., Granados, G. M., Shuey, L., Barnes, I., Wingfield, M. J., and McTaggart, A. R. 2016. A unique genotype of the rust pathogen, *Puccinia psidii*, on Myrtaceae in South Africa. Australas. Plant. Pathol. 45:645-652.

Santos, S. A., Vidigal, P. M. P., Guimaraẽs, L. M. S., Mafia, R. G., Templeton, M. D., and Alfenas, A. C. 2020. Transcriptome analysis of *Eucalyptus grandis* genotypes reveals constitutive overexpression of genes related to rust (*Austropuccinia psidii*) resistance. Plant Mol. Biol. 104: 339-357.

Sekiya, A., Marques, F. G., Leite, T. F., Cataldi, T. R., de Moraes, F. E., Pinheiro, A. L. M., Labate, M. T. V., and Labate, C. A. 2021. Network analysis combining proteomics and metabolomics reveals new insights into early responses of *Eucalyptus grandis* during rust infection. Front. Plant Sci. 11: 604849.

Soewarto, J., Giblin, F., and Carnegie, A. J. 2019. *Austropuccinia psidii* (myrtle rust) global host list. Version 4. Australian Network for Plant Conservation, Canberra, ACT. http://www.anpc.asn.au/myrtle-rust

Sonesone, C., Love, M. I., and Robinson, M. D. 2015. Differential analyses or RNA-seq: Transcript-level estimates improve gene-level inferences. F1000Research 4:1521.

Song, X., Rampitsch, C., Soltani, B., Mauthe, W., Linning, R., Banks, T., McCallum, B., and Bakkeren, G. 2011. Proteome analysis of wheat leaf rust fungus, *Puccinia triticina,* infection structures enriched for haustoria. Proteomics 11:944-963.

Swanepoel, S., Oates, C. N., Shuey, L. S., Pegg, G. S., and Naidoo, S. 2021. Transcriptome analysis of *Eucalyptus grandis* implicates brassinosteroid signaling in defense against myrtle rust (*Austropuccinia psidii*). Front. For. Glob. Change 4:778611.

Tiwari, S., Thankur, R., and Shankar, J. 2015. Role of heat-shock proteins in the cellular function and in the biology of fungi. Biotechno1. Res. Int. 2015:132635.

Tobias, P. A., Guest, D. I., Külheim, C., and Park, R. F. 2018. De novo transcriptome study identifies candidate genes involved in resistance against *Austropuccinia psidii* (myrtle rust) in *Syzygium luehmannii* (riberry). Phytopathology 108:627-640.

Tobias, P. A., Schwessinger, B., Deng, C. H., Wu, C., Dong, C., Sperschneider, J., Jones, A., Lou, Z., Zhang, P., and Sandhu, K. S. 2021. *Austropuccinia psidii,* causing myrtle rust, has a gigabase-sized genome shaped by transposable elements. G3: Genes. Genom. Genet. 11:jkaa015.

Uchida, J., Zhong, S., and Killgore, E. 2006. First report of a rust disease on Ohia caused by *Puccinia psidii* in Hawaii. Plant Dis. 90:524.

Urban, M., Cuzick, A., Seager, J., Wood, V., Rutherford, K., Venkatech, S. Y., De Silva, N., Martinez, M. C., Pedro, H., Yates, A. D., Hassani-Pak, K., and Hammond-Kosack, K. E. 2020. PHI-base: The pathogen−host interactions database. Nucleic Acids Res. 48:D613-D620.

Wu, W., Nemri, A., Blackman, L. M., Catanzariti, A.-M., Sperschneider, J., Lawrence, G. J., Dodds, P. N., Jones, D. A., and Hardham, A. R. 2019. Flax rust infection transcriptomics reveals a transcriptional profile that may be indicative for rust *Avr* genes. PLoS One 14:e0226106.

Xie, F., Li, G., Wang, Y., Zhang, Y., Zhou, L., Wang, C., Liu, S., Liu, S., and Wang, C. 2017. Pyridoxal phosphate synthases PdxS/PdxT are required for *Actinobacillus pleuropneumoniae* viability, stress tolerance and virulence. PLoS One 12:e0176374.

Young, M. D., Wakefield, M. J., Smyth, G. K., and Oshlack, A. 2010. Gene ontology analysis for RNA-seq: Accounting for selection bias. Genome Biol. 11:R14.

Zhuang, J. Y., and Wei, S. X. 2011. Additional materials for the rust flora of Hainan Province. China. Mycosystem 30:853-860.